

B. Fatigue and Wear

INFLUENCE OF MICROSTRUCTURE ON THE FATIGUE BEHAVIOR OF Ti-6Al-4V

M. Peters, A. Gysler*, and G. Luetjering

Ruhr-University Bochum, West-Germany

* German Aerospace Research Establishment (DFVLR),
Cologne, West-Germany

Introduction

There is general agreement in the literature and enough experimental evidence that refining the microstructure of the Ti-6Al-4V alloy results in an improvement of fatigue strength of smooth specimens[1-4]. But it was also pointed out that this effect cannot be separated in many cases from a texture effect[5,6]. Experimental evidence exists that variations in texture affect the fatigue strength of Ti-6Al-4V but in comparing different texture types the microstructure was also changed[6-8]. Recently, it has been shown on Ti-6Al-4V that texture and microstructure can be controlled separately to a large extent[9], which offers the possibility to investigate the individual effects of texture (at constant microstructure) and of microstructure (at constant texture) on the mechanical properties. Taking this approach it was tried in the present work to investigate the influence of α -grain size in equiaxed microstructures on the fatigue strength keeping the texture constant. As comparison also a so-called bi-modal microstructure consisting of primary equiaxed α -grains in a lamellar matrix was investigated to show the effect of separating the highly textured α -grains from each other. Since it is known from binary Ti-Al alloys[10,11] that the grain size has opposite effects on nucleation and propagation of fatigue cracks propagation tests were also performed. Furthermore, to be able to separate microstructural and environmental effects on the fatigue strength in laboratory air additional tests were done in vacuum and NaCl solution.

Experimental Procedure

The material investigated had the following composition: 6.4%Al, 4.0%V, 0.19% oxygen (wt.-%). The alloy was made by TIMET and forged in the β -phase field to a plate thickness of 30mm by Ladish Company. The starting heat treatment for all specimens was 15 min at 1050°C followed by water-quenching. To ascertain a constant texture the deformation process was the same for all specimens: cross-rolling ($\phi = -1.4$) at 800°C. After water-quenching from 800°C the specimens were heat treated differently to achieve the different microstructures. The final heat treatment was again the same for all specimens: 1 hour at 800°C followed by water-quenching, aging at 500°C for 24h and air-cooling. All heat treatments were done in an argon atmosphere.

Tensile tests were performed on round specimens with a gage length of 20mm and a diameter of 4mm using a strain rate of $8.3 \times 10^{-4} \text{ s}^{-1}$.

Fatigue life curves were measured on round smooth specimens with a diameter of 2mm. The surface of the specimens was polished electrolytically.

The tests were done with a frequency of 80 Hz under stress controlled push-pull ($R = -1$) conditions. The crack nucleation mechanism was investigated on slightly etched specimens by SEM.

Fatigue crack propagation measurements were carried out with a frequency of 10 Hz on CT type specimens (40 x 40 x 6mm) at $R = 0.2$. The crack length was measured optically with a travelling microscope.

The fatigue life curves as well as the fatigue crack propagation rates were determined in three different environments: vacuum (better than 10^{-4} Pa), laboratory air (about 50% relative humidity), and 3.5% NaCl solution under open circuit conditions at the free corrosion potential.

All specimens for mechanical tests were machined before the last aging treatment at 500°C for 24 hours. The stress axis was always parallel to the rolling direction. All mechanical tests were performed at room temperature.

Results and Discussion

1. Characterization of microstructure and texture

The three different microstructures investigated are illustrated in Figures 1-3 by light and transmission electron micrographs. A fine equiaxed structure was developed by annealing the material after deformation for 1 hour at 800°C (Figure 1). The α -grain size was about 2 μ m as can be seen from the transmission electron micrograph (Figure 1b) and the microstructure was uniform equiaxed (Figure 1a). A coarser equiaxed microstructure with an average α -grain size of about 12 μ m was developed by a long annealing time (96 hours) at 800°C (Figure 2). In both equiaxed structures the β -phase was located mainly at α -grain boundary triple points. A bi-modal microstructure consisting of isolated primary α -grains in a fine lamellar matrix (Figure 3) was achieved by annealing the deformed material for 1 hour at 955°C followed by water-quenching and annealing for 1 hour at 800°C. The equiaxed β -grains present at 955°C transformed first martensitically upon quenching and then at 800°C into the fine lamellar structure. The average size of the primary equiaxed α -grains was about 6 μ m. The final aging treatment at 500°C for 24 hours precipitated in all three microstructures Ti_3Al -particles in the α -phase and fine α -particles in the β -phase[12].

The equiaxed α -phase exhibited in all three microstructures the same texture which was formed already during the cross-rolling deformation process at 800°C and which did not change significantly during the subsequent different heat treatments. The type of texture is illustrated in Figure 4 on the fine equiaxed microstructure as an example. The coarse equiaxed and the bi-modal structures had virtually the same texture. From the (0002) pole figure it can be seen that the basal planes were nearly parallel to the rolling plane. The angle between rolling plane and basal planes was about 20°. It should be pointed out that the α -phase of the fine lamellar portions of the bi-modal structure does not have a pronounced texture[13].

2. Tensile tests

The results of the tensile tests are listed in Table 1. As expected, the modulus of elasticity did not change by varying the α -grain size of the equiaxed microstructure from 2 to 12 μ m. The relative low value of 109 GPa is a result of the texture type[9] having the basal planes nearly parallel to the stress axis. The modulus for the bi-modal microstructure was higher

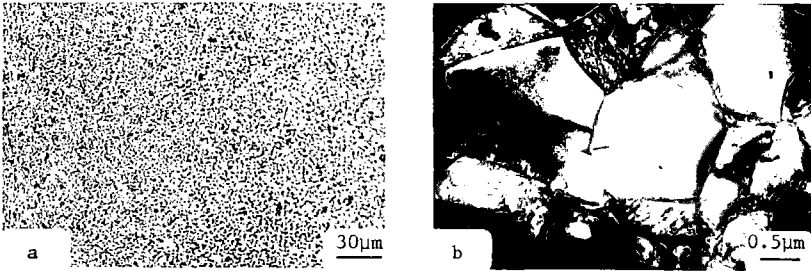


Figure 1: Fine equiaxed microstructure: a) LM, b) TEM.
 15 min 1050°C/WQ, $\phi = -1.4$ at 800°C/WQ,
 1h 800°C/WQ, 24h 500°C/AC

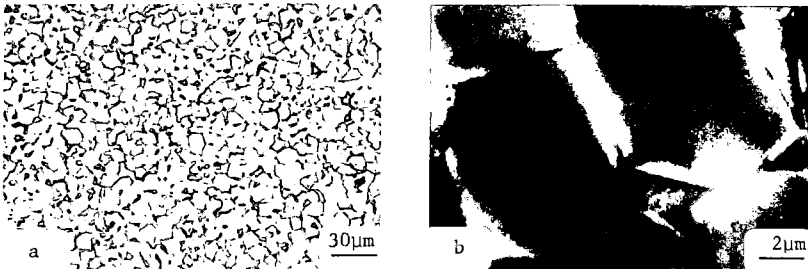


Figure 2: Coarse equiaxed microstructure: a) LM, b) TEM.
 15 min 1050°C/WQ, $\phi = -1.4$ at 800°C/WQ,
 96h 800°C/WQ, 24h 500°C/AC.

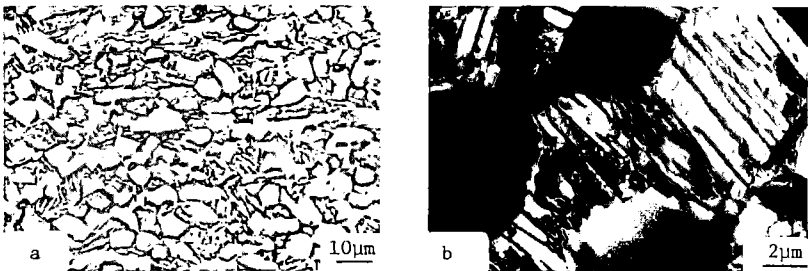


Figure 3: Bi-modal microstructure: a) LM, b) TEM.
 15 min 1050°C/WQ, $\phi = -1.4$ at 800°C/WQ,
 1h 955°C/WQ, 1h 800°C/WQ, 24h 500°C/AC.

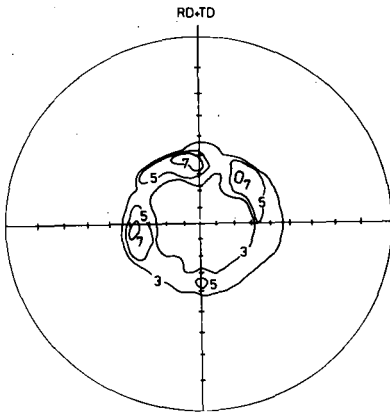


Figure 4: BASAL texture type by cross-rolling, (0002) pole figure. 15 min 1050°C/WQ, $\phi = -1.4$ at 800°C/WQ, 1h 800°C/WQ.

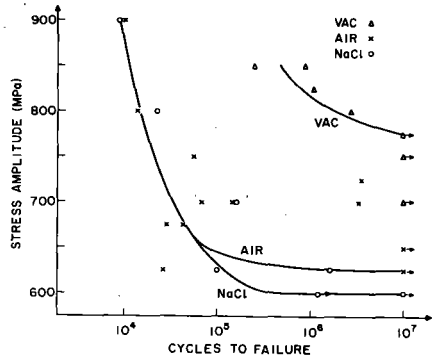


Figure 5: Fine equiaxed microstructure: Fatigue life curves in vacuum, laboratory air, and 3.5% NaCl solution.

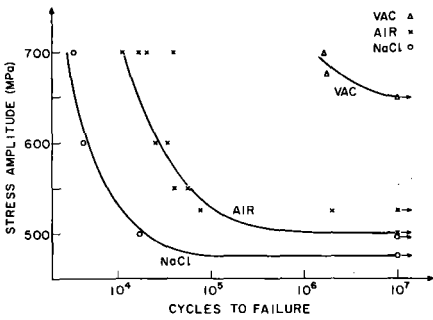


Figure 6: Coarse equiaxed microstructure: Fatigue life curves in vacuum, laboratory air, and 3.5% NaCl solution.

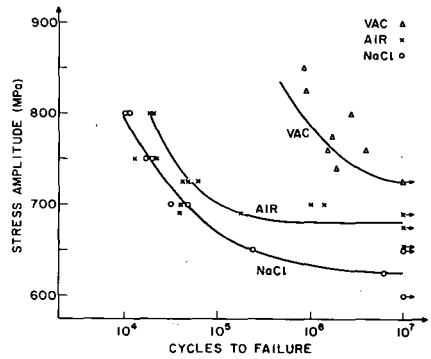


Figure 7: Bi-modal microstructure: Fatigue life curves in vacuum, laboratory air, and 3.5% NaCl solution.

due to the "texture-free" fine lamellar portions of the structure. For comparison, specimens of this alloy with an entirely fine lamellar structure (15 min 1050°C/WQ, 1h 800°C/WQ, 24h 500°C/AC) had a modulus of 119 GPa[13]. This is only a qualitative indication because the solute content of both lamellar structures is not quite the same.

Table 1: Tensile Properties

	E (GPa)	$\sigma_{0.2}$ (MPa)	σ_F (MPa)	ϵ_F
Fine equiaxed	109	1120	1505	0.70
Coarse equiaxed	109	1030	1370	0.56
Bi-modal	114	1005	1455	0.61

The yield stress increased by about 100MPa by reducing the α -grain size of the equiaxed microstructure from 12 μ m to 2 μ m. The value for the bi-modal structure with an α -grain size of 6 μ m was even lower than that of the coarse equiaxed structure. This again can be attributed to the lamellar portions of the structure because the yield stress of specimens with an entirely fine lamellar structure was 985MPa. It should be noted that the yield stress level for all three microstructures was very high as a result of the aging treatment at 500°C for 24 hours.

The fracture stresses and true fracture strains were also very high for all three conditions. This is due to the relative small α -grain size values of all three microstructures[14]. Noteworthy is the high ductility of the bi-modal structure taking into account the low fracture values for specimens with entirely lamellar microstructure ($\sigma_F = 1250$ MPa, $\epsilon_F = 0.26$). A possible explanation is the much smaller α -plate length in the lamellar portions of the bi-modal structure (Figure 3b), which is limited by the β -grain size of the two phase micro-duplex structure at 955°C, as compared to the martensitic plate dimensions commonly obtained in Ti-6Al-4V β -quenched microstructures.

3. Fatigue life tests,

The results of the fatigue life tests for the three different microstructures are shown in Figures 5-7. The fine equiaxed structure (Figure 5) exhibited a very high fatigue strength in vacuum. A drastic drop in fatigue strength occurred when the material was tested in laboratory air. Not much difference was found between tests in laboratory air and in 3.5% NaCl solution. This is in agreement with the literature[15] and was ascribed to the insensitivity of the Ti-6Al-4V alloy to this kind of aggressive environments. The large drop in fatigue strength between tests in vacuum and laboratory air suggests that already laboratory air is as aggressive as NaCl solution and that the Ti-6Al-4V alloy in this microstructural condition is very sensitive to the moisture content of the environment. This might also explain the large scatter in fatigue life observed for tests in laboratory air (Figure 5).

The same general tendency was found for the coarse equiaxed microstructure (Figure 6) except that the fatigue strength at 10^7 cycles was more than 100MPa lower than the value for the fine equiaxed structure. A different behavior was observed for the bi-modal microstructure (Figure 7). No large

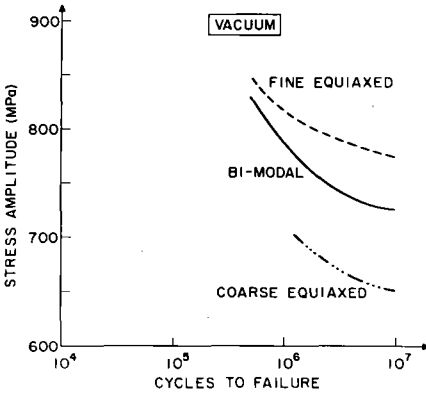


Figure 8: Comparison of fatigue strength in vacuum.

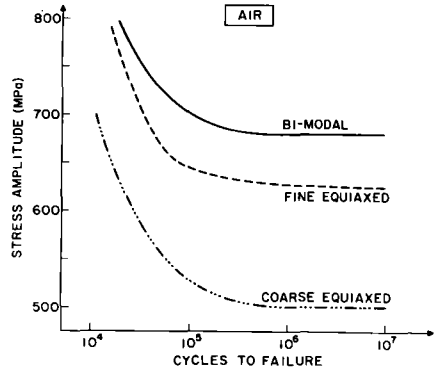


Figure 9: Comparison of fatigue strength in laboratory air.

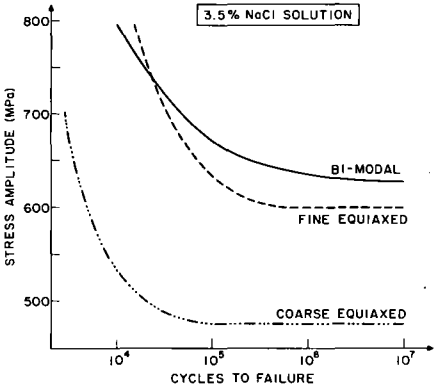


Figure 10: Comparison of fatigue strength in 3.5% NaCl solution.

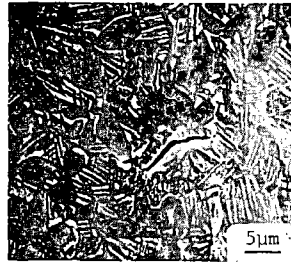


Figure 11: Bi-modal microstructure: Fatigue crack nucleation in primary α -phase, (SEM).

drop in fatigue strength between tests in vacuum and laboratory air was present and the total difference between vacuum and 3.5% NaCl solution was only about 100MPa as compared to the equiaxed structures which show a difference of 175MPa. These results suggest, that the bi-modal microstructure is less sensitive to the aggressive environments tested (laboratory air, NaCl solution).

The fatigue life data are replotted in Figures 8-10 to allow a better comparison of the three different microstructures. The results in vacuum (Figure 8) show the effect of microstructure without any interference of environment. The fatigue strength increased with decreasing primary α -grain size. Comparing the three microstructures in laboratory air and 3.5% NaCl solution (Figures 9 and 10) it can be seen that the ranking changed. The bi-modal structure with a primary α -grain size of $6\mu\text{m}$ was now even superior to the fine grained ($2\mu\text{m}$) equiaxed material. This better performance of the bi-modal structure is only due to a lower sensitivity to aggressive environments.

The investigation of the crack nucleation mechanisms by SEM showed that as expected the cracks nucleated in the equiaxed structures at slip bands in the α -phase intersecting the specimen surface. For the bi-modal microstructure the investigation of many small cracks led to the conclusion that the cracks also nucleated in slip bands in the primary α -grains and propagated as much as possible within the primary α -phase. An example of a small microcrack with a length of about $15\mu\text{m}$ is shown in Figure 11.

4. Fatigue crack propagation tests

Fatigue crack propagation rates were measured in the range between 10^{-9} and 10^{-7}m/cycle in vacuum, laboratory air, and 3.5% NaCl solution. The results are shown in Figures 12-14. The vacuum tests revealed that the coarse equiaxed microstructure exhibited a slower crack propagation rate than the fine equiaxed structure (Figure 12). The bi-modal structure showed the slowest crack propagation rate. This cannot be explained by a grain size effect alone[11] because the primary α -grain size of the bi-modal structure was only $6\mu\text{m}$ and therefore smaller than the α -grain size of the coarse equiaxed microstructure ($12\mu\text{m}$). The reason for the slower crack propagation rate of the bi-modal structure is probably due to the lamellar portions of the structure. It is well known that lamellar structures exhibit slower crack propagation rates as compared to equiaxed structures which is generally explained by more crack branching in lamellar structures[4].

In the presence of an aggressive environment, laboratory air (Figure 13) and 3.5% NaCl solution (Figure 14), the crack propagation rates were faster and the differences between the three microstructures became smaller. It should be noted that in 3.5% NaCl solution the fine and coarse equiaxed microstructures showed the same crack propagation rates at low ΔK -values. For other texture types the fine equiaxed structure can be even better in 3.5% NaCl solution than the coarse equiaxed structure[13]. The results indicate that coarse equiaxed microstructures exhibit a better intrinsic fatigue crack propagation behavior but that the propagation rates are more accelerated by aggressive environments as compared to fine structures.

It should be further noted that for all three microstructures a large increase in propagation rate was present when going from vacuum to laboratory air but only a slight increase in propagation rate existed when comparing

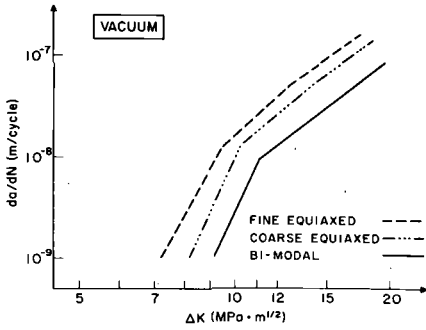


Figure 12: Comparison of fatigue crack propagation rates in vacuum.

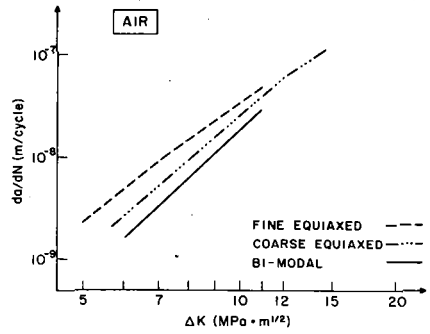


Figure 13: Comparison of fatigue crack propagation rates in laboratory air.

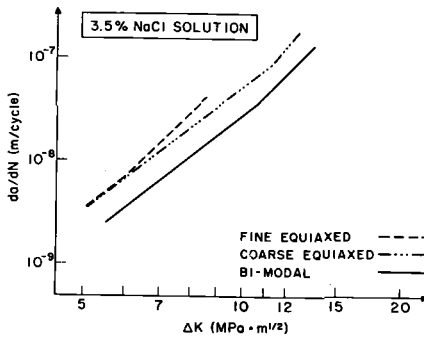


Figure 14: Comparison of fatigue crack propagation rates in 3.5% NaCl solution.

laboratory air and 3.5% NaCl solution. This again shows that laboratory air is already a strong aggressive environment for the Ti-6Al-4V alloy.

Conclusions

1. The fatigue strength of Ti-6Al-4V can be improved by reducing the α -grain size of equiaxed microstructures.
2. For a high fatigue strength in aggressive environments it is advantageous to separate the α -grains by fine lamellar portions (bi-modal microstructure) especially if the primary α -phase is highly textured.
3. Laboratory air is already a very aggressive environment for the Ti-6Al-4V alloy, because a large drop in fatigue strength and a large increase in fatigue crack propagation rate existed when comparing tests in vacuum and in laboratory air. The difference between laboratory air and 3.5% NaCl was small.
4. Equiaxed and bi-modal microstructures with small α -grain sizes can be aged to high yield stress levels without losing the high ductility and the high fatigue strength.
5. For an application of the Ti-6Al-4V alloy involving fatigue in aggressive environments it is recommended to use a bi-modal microstructure with a small primary α -grain size (smaller than 10 μ m)[16].

Acknowledgment

The assistance of I. Moritz and K. Rittner at the Ruhr-University Bochum and of J. Endrejat and H. Bellingradt at the DFVLR in the experimental work is gratefully acknowledged. This work was supported by the Electric Power Research Institute, Palo Alto, under contract RP 1266-1.

References

1. J. J. Lucas: Titanium Science and Technology, 3 (1973), 2081, Plenum Press, New York.
2. A. W. Bowen and C. A. Stubbington: Titanium Science and Technology, 3 (1973), 2097, Plenum Press, New York.
3. C. A. Stubbington and A. W. Bowen: Titanium Science and Technology, 2 (1973), 1283, Plenum Press, New York.
4. N. E. Paton, J. C. Williams, J. C. Chesnutt, and A. W. Thompson: AGARD-CP-185, (1975), 4-1.
5. A. W. Bowen: Scripta Met., 11 (1977), 17.
6. A. W. Bowen: Titanium Science and Technology, 2 (1973), 1271, Plenum Press, New York.
7. F. Larson and A. Zarkades: MCIC-74-20, (1974), Battelle, Columbus.
8. A. W. Sommer and M. Creager: AFML-TR-76-222, (1977).
9. M. Peters and G. Luetjering: Proc. Fourth Intern. Conf. on Titanium, (1980), Kyoto, Japan.
10. A. Gysler, J. Lindigkeit, and G. Luetjering: Proc. Fifth ICSMA, 2 (1979), 1113, Aachen, West-Germany.
11. J. Lindigkeit, G. Terlinde, A. Gysler, and G. Luetjering: Acta Met., 27 (1979), 1717.
12. G. Welsch, G. Luetjering, K. Gazioglu, and W. Bunk: Met. Trans., 8A (1977), 169.
13. M. Peters: Ph.D. - Thesis, (1980), Ruhr-University Bochum.

14. G. Terlinde, A. Gysler, and G. Luetjering: Proc. Third Intern. Conf. on Titanium, (1976), Moscow, USSR, in press.
15. R. I. Jaffee: Met. Trans., 10A (1979), 139.
16. R. I. Jaffee, G. Luetjering, and T. Rust: Proc. Fourth Intern. Conf. on Titanium, (1980), Kyoto, Japan.